

# Experimental Characterization of Two-Phase Flow Instability Thresholds in Helically Coiled Parallel Channels

Davide Papini, Marco Colombo, Antonio Cammi, Marco E. Ricotti  
Politecnico di Milano, Department of Energy, Nuclear Engineering Division - CeSNEF  
Via La Masa 34, 20156 Milano, Italy  
Tel: +39 02 2399 6333, Fax: +39 02 2399 8566, Email: [davide.papini@mail.polimi.it](mailto:davide.papini@mail.polimi.it)

Dario Colorado  
Centro de Investigación en Ingeniería y Ciencia  
Aplicadas (CIICAp), Universidad Autónoma del Estado  
de Morelos (UAEM)  
Av. Universidad 1001, Col. Chamilpa, 62209  
Cuernavaca, Morelos, México

Matteo Greco, Gaetano Tortora  
SIET, S.p.A.  
Via Nino Bixio 27/c, 29121, Piacenza, Italy

**Abstract** – Among the various types of instabilities affecting vapor generation in boiling systems, Density Wave Oscillation (DWO) occurrence within parallel channels is depicted. Parallel channel instability may represent a critical concern for the operation and safety of the once-through steam generators adopted in GenIII+ and GenIV nuclear reactor concepts. Extensive attention is required to determine the safe operating regime of a two-phase heat exchanger, by evaluating the instability threshold values of system parameters such as thermal power, flow rate, pressure, inlet temperature and exit quality.

While the amount of published experimental work in the field of DWOs investigation in parallel straight tubes is overwhelming since the '60, scarce attempt has been dedicated to the helical-coiled tube geometry. Conversely, coiled pipes are foreseen for applications to steam generators of the next generation NPPs, due to compactness and higher efficiency in heat transfer.

The paper deals with the results of an experimental campaign on flow instability occurrence in two electrically heated helically coiled parallel tubes. In the framework of the IRIS project, a full-scale open-loop experimental facility simulating the thermal-hydraulic behavior of a helically coiled steam generator has been built and operated at SIET labs in Piacenza (Italy). The facility comprises two helical tubes (1 m coil diameter, 32 m length, 8 m height), connected via lower and upper headers. In order to excite flow unstable conditions starting from stable operating conditions, supplied electrical power was gradually increased up to the appearance of permanent and regular flow oscillations. Several flow instability threshold conditions were identified, in a test matrix of pressures (80 bar, 40 bar, 20 bar), mass fluxes (600 kg/m<sup>2</sup>s, 400 kg/m<sup>2</sup>s, 200 kg/m<sup>2</sup>s), and inlet subcooling (from -30% up to ~0). The long test section feature and the helical-coiled tube geometry render the present facility a quite unique test case in the outline of two-phase flow instability experimental studies. Parametric effects of the operating pressure, flow rate and inlet subcooling on the threshold power are discussed. The period of oscillations is also discussed.

## I. INTRODUCTION

The new reactor projects of Generation III+ and Generation IV raise in the nuclear field the demand for new technological solutions to improve the reactor safety through simpler designs. In this framework, rapidly growing is the interest on integral Small-medium Modular Reactors (SMRs), where all the primary system components are located inside the reactor vessel. The

integral layout permits to reduce by design risks and effects of different postulated accidents, such as large releases of primary coolant (large break LOCA accidents).

New reactor concepts also rely on improvement in single plant components. In nuclear systems, one of the critical components is the Steam Generator (SG). The adoption of helical and spiral tubes is envisaged in the SGs of different reactor projects of Generation III+ and Generation IV. As a matter of fact, helical geometry results

in more compact SG – fitting with the integral layout – and efficiency improvement through better heat transfer characteristics. Helically coiled tubes have been adopted in different industrial fields (ranging from fossil fuelled power plants, natural gas liquefaction apparatus, to solar energy concentrator receivers), including applications within nuclear reactors, even though in few particular cases. However, more research work is needed to deepen the knowledge of physics of two-phase flows in helical geometry.

The Nuclear Engineering Division of the Department of Energy (Politecnico di Milano) is involved in thermal-hydraulic studies concerning two-phase flows in components of new generation nuclear reactors<sup>1,2</sup>. The attention is focused on helical tube SGs for SMRs. In particular, this paper deals with an experimental activity dedicated to boiling instability occurrence in helical parallel channels. A full-scale open-loop experimental facility simulating the thermal-hydraulic behavior of a helically coiled SG was installed and operated at SIET labs in Piacenza. The facility comprises two helical tubes representing the SG of an integral Pressurized Water Reactor (PWR) of Generation III+, connected via lower and upper headers.

Density Wave Oscillations (DWOs) are investigated as the main “dynamic type” instability mode<sup>3</sup>. The classical interpretation of the phenomenon ascribes the origin of the instability to waves of “heavier” and “lighter” fluids<sup>3</sup>, and respective delays through the channel. The difference in density between the fluid entering the heated channel (subcooled liquid) and the fluid exiting (low density two-phase mixture) triggers delays in the transient distribution of pressure drops along the tube, which may lead to self-sustained oscillations (with single-phase and two-phase pressure drops oscillating in counter-phase). A constant-pressure-drop boundary condition (commonly provided by two or more parallel channels) is required to excite the flow rate perturbations at the inlet of the boiling channel.

DWOs and more generally two-phase flow instabilities have been studied since the '60. The large amount of theoretical and experimental works on the subject is collected in different literature reviews<sup>3,4</sup>. A large number of experimental researches is available, the majority of which dealing indeed with straight tubes and few meters long test sections. Amongst them, a systematic study on the onset and the frequency of this type of oscillations at various system conditions is provided by Saha et al.<sup>5</sup> using a uniformly heated single boiling channel with bypass, and by Masini et al.<sup>6</sup> working with two vertical parallel tubes. To the best of Authors knowledge, scarce number of experiments was conducted studying full-scale long test sections, and no data are available on helically coiled tube geometry.

In this frame, the experimental activity described in this work presents the unique feature to investigate the

influence of the helical shape (through the centrifugal field induced by tube bending) on instability occurrence, as well as to provide a useful experimental database for model validation. Moreover, the influence of a long test section on instability thresholds is depicted.

Section II describes the experimental facility, the test matrix and the experimental procedure adopted to reach the onset of instability. Section III presents the distinctive features of DWOs, whereas the experimental stability maps are shown in Section IV. Some considerations are made on the period of oscillations and period of oscillations to transit time ratio. Finally, the effect of inlet throttling and the appearance of Ledinegg type instability – given by the constant-pressure-drop boundary condition during the execution of some test runs – are briefly presented.

## II. THE EXPERIMENTAL FACILITY

The experimental facility, built and operated at SIET labs, is an extension of an electrically heated test section used for the study of the thermal-hydraulics of a helically coiled SG tube (two-phase pressure drops – under diabatic and adiabatic conditions – and dryout thermal crisis occurrence)<sup>1</sup>. In the framework of the IRIS (International Reactor Innovative and Secure) project, the same test section was also included in a closed loop circuit, to study a passive heat removal system with natural circulation<sup>2</sup>. The facility, provided with SG full elevation and suited for prototypical thermal-hydraulic conditions reproduction, implements the common simplification given by a constant heat flux boundary – via electrical power – instead of real controlled-temperature boundary. When dealing with experiments on instability phenomena, despite different dynamic responses, such different boundary is expected to secondarily affect the instability threshold (as the instability inception is induced by the specific thermal power supplied, owing to the reached thermodynamic quality).

Coil diameter (1 m) has been chosen as representative of a mean value of IRIS steam generator tube, while tube inner diameter (12.53 mm) is the commercially scheduled value nearer to IRIS real value (13.24 mm). The heated tube is thermally insulated by means of rock wool. Thermal losses were measured via runs with single-phase hot pressurized water flowing inside the steam generator, and estimated as a function of the temperature difference between external tube wall and the environment.

The facility was renewed to test DWOs in parallel channels, by adding a second helical tube identical to the first one (same coil diameter, pitch and length). The two helices have been connected with common lower and upper headers to provide the constant-pressure-drop boundary condition required for the instability inception. The conceptual sketch of the new facility is depicted in Fig. 1, whereas a global view is provided in Fig. 2. Geometrical data of the two helical tubes are listed in Table I.

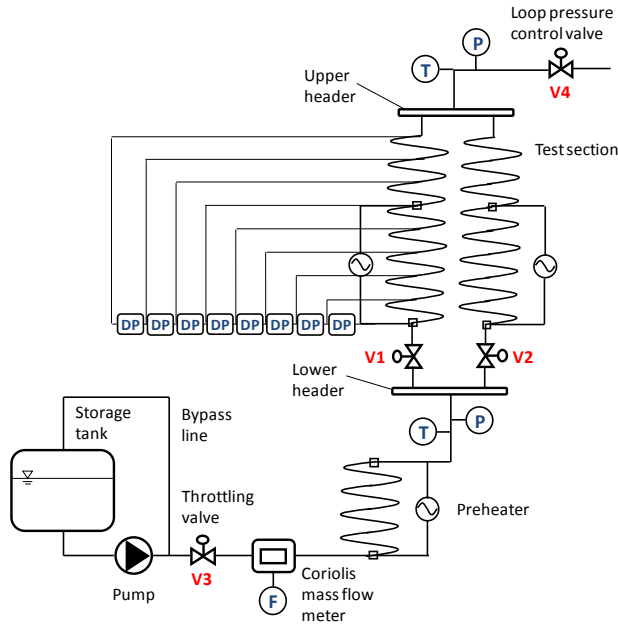


Fig. 1. Sketch of the experimental facility installed at SIET labs.

The whole facility is made by a supply section and a test section. The supply section feeds demineralized water from a tank to the test section, by means of a centrifugal booster pump and a feed water pump, i.e. a volumetric three cylindrical pump with a maximum head of about 200 bar.

The flow rate is controlled by a throttling valve (V3) positioned downwards the feed water pump and after a bypass line. System pressure control is accomplished by acting on a throttling valve (V4) placed at the end of the steam generator.

An electrically heated preheater is located before the test section, and allows creating the desired temperature at the inlet of the test section. The test section is electrically heated via Joule effect by DC current. Two distinct, independently controllable and contiguous sections are provided. For instability experiments, power was supplied only to the first section (24 m), instead the second section (8 m) worked as a riser unheated section.

TABLE I

Test section main data.

|                            |              |
|----------------------------|--------------|
| Tube material              | SS AISI 316L |
| Tube inner diameter [mm]   | 12.53        |
| Tube outer diameter [mm]   | 17.24        |
| Coil diameter [mm]         | 1000         |
| Coil pitch [mm]            | 800          |
| Tube length [m]            | 32           |
| Heated section length [m]  | 24           |
| Riser length [m]           | 8            |
| Steam generator height [m] | 8            |



Fig. 2. Global view of the facility test section.

Each tube is provided at inlet with a calibrated orifice (with a differential pressure transmitter) used to measure the flow rate in each channel and to visually detect the instability inception, and with a valve to impose a concentrated pressure drop. V1 and V2 represent the total pressure drop (instrumented orifice + valve) introduced at the inlet of the two helical tubes, respectively.

The water pressures at inlet and outlet headers are measured by absolute pressure transducers; nine pressure taps are disposed nearly every 4 m along one tube and eight differential pressure transducers connect the pressure taps. Detailed distances between the taps are reported in Table II. An accurate measurement of the total flow rate is obtained by a Coriolis flow-meter, placed between the pump and the preheater. Bulk temperatures are measured with K-class thermocouples drowned in a small well at SG inlet and outlet headers. Wall thermocouples (K-class) are mounted throughout the two coils, with fining near the ends to identify the risk of dryout occurrence. Electrical power is obtained via separate measurement of current (by a shunt) and voltage drop along the test section by a voltmeter.

TABLE II

Pressure taps distribution along the test section (Channel A).

|                              | Tap 1 | Tap 2 | Tap 3 | Tap 4 | Tap 5 |
|------------------------------|-------|-------|-------|-------|-------|
| Distance from tube inlet [m] | 0.20  | 5.17  | 9.19  | 13.15 | 17.14 |
|                              | Tap 6 | Tap 7 | Tap 8 | Tap 9 |       |
| Distance from tube inlet [m] | 21.64 | 25.59 | 29.09 | 32.06 |       |

All the measurement devices have been tested and calibrated at the certified SIET labs. A summary of the uncertainties is reported in Table III.

TABLE III

List of the uncertainties of physical quantities (referred to measurement values).

|                                 |                                   |
|---------------------------------|-----------------------------------|
| Water flow rate                 | $\pm 1\%$                         |
| Fluid bulk and wall temperature | $\pm 0.7\text{ }^{\circ}\text{C}$ |
| Absolute pressure               | $\pm 0.1\%$                       |
| Differential pressure           | $\pm 0.4\%$                       |
| Supplied electrical power       | $\pm 2.5\%$                       |
| Evaluated thermal losses        | $\pm 15\%$                        |

### II.A. Range of Explored Variables

DWOs result from multiple feedback effects between the flow rate, the vapor generation rate and the pressure drops in the boiling channel. To fully describe the stable region of the system and collect information on instability phenomena, it is necessary to determine instability thresholds in a wide range of system operating parameters.

A thorough test matrix was prepared to study the effects of system pressure, mass flow rate and inlet subcooling on system stability, by investigating:

- 3 levels of pressure: 80 bar, 40 bar and 20 bar;
- 3 levels of mass flux: 600 kg/m<sup>2</sup>s, 400 kg/m<sup>2</sup>s and 200 kg/m<sup>2</sup>s;
- several values of inlet subcooling between  $x_{in} = -30\%$  and  $x_{in} = 0\%$ .

The entire test matrix was executed with reference to a “basically open” configuration of the inlet valves V1 and V2 (corresponding valve loss coefficient  $k_{in} = 45$ ). The effect of inlet throttling was at last studied by progressively closing the valves and repeating the stability map at  $P = 40$  bar and  $G = 400$  kg/m<sup>2</sup>s.

### II.B. Experimental Procedure

It was decided to act on the electrical power supplied to the test section in order to reach flow unstable conditions starting from a stable operating system. In every test run, the heating power was gradually increased from nominal values up to the appearance of flow instability.

The adopted test procedure can be summarized in the following steps:

- (1) Registration of the gravitational head of the different instruments.
- (2) Characterization of the normal behavior of the system (for instance, check that, at open V1 and V2 valves, the flow rate is reasonably balanced between the two coils).

- (3) Impose the defined position of V1 and V2 valves.
- (4) Define pressure level.
- (5) Impose a value of flow rate.
- (6) Impose a value of inlet subcooling by means of the preheater.
- (7) Reach the desired pressure level by generating vapor with power increase. When the desired pressure is obtained, keep the system in a steady-state condition (measurements of temperature, pressure, flow rate and heat input).
- (8) The electrical power is progressively increased by small amounts (small steps of 2-5 kW per tube), until sustained oscillations are observed (check that the system pressure remains more or less constant).
- (9) Once the instability is recorded, take the system back to step 6, and change the subcooling. Repeat steps 7 and 8 up to the instability (same operating pressure).
- (10) Once all the subcooling values are tested for a flow rate level, change the flow rate and repeat steps 6-9.
- (11) Once all the flow rate values defined in step 5 are completely explored (every subcooling value), change the desired pressure level and repeat steps 5-10.

## III. DWO CHARACTERIZATION

DWO appearance in a boiling channel can be detected by monitoring the flow rate, which starts to oscillate when power threshold is reached. The calibrated orifices installed at the inlet of both tubes permit to measure the flow rate through the recording of the pressure drops established across them. Thus, flow instability power threshold was experimentally defined as the power corresponding to permanent and regular flow oscillations, detected by visual observation of the pressure drop recording of the calibrated orifices (within V1 and V2 of Fig. 1). The system was considered completely unstable when flow rate oscillation amplitude reached the 100% of its steady-state value. Obviously, flow rate in the two channels oscillates in counter-phase, being the total system mass flow rate imposed, as it is shown in Fig. 3, where fully developed DWOs are depicted. The “square wave” shape of the curves is due to the reaching of instruments full scale.

Data collected during instability inception and fully developed instability allowed understanding the distinctive features of DWOs.

Total pressure drops across the tubes oscillate in counter-phase too (Fig. 4). Conversely, the system pressure oscillates with a frequency that is double if compared with the frequency of pressure drop oscillations (Fig. 5).

Counter-phase oscillation of single-phase and two-phase pressure drops within each channel is known to be one of the triggering events leading to the appearance of DWOs. Fig. 6 compares the pressure drops between pressure taps placed on different regions of Channel A (according to the distribution depicted in Table II), in case of self-sustained instability. Pressure drops in the single-phase region (DP 2-3) oscillate in counter-phase with respect to two-phase pressure drops (DP 6-7 and DP 8-9). The phase shift is not abrupt, but it appears gradually along the channel. As a matter of fact, the pressure term DP 4-5 (low-quality two-phase region) shows only a limited phase shift with respect to single-phase zone (DP 2-3).

Moreover, large amplitude fluctuations in channel wall temperatures, so named “thermal oscillations”<sup>4</sup>, always occur (Fig. 7), associated with fully developed density wave oscillations that trigger intermittent film boiling conditions.

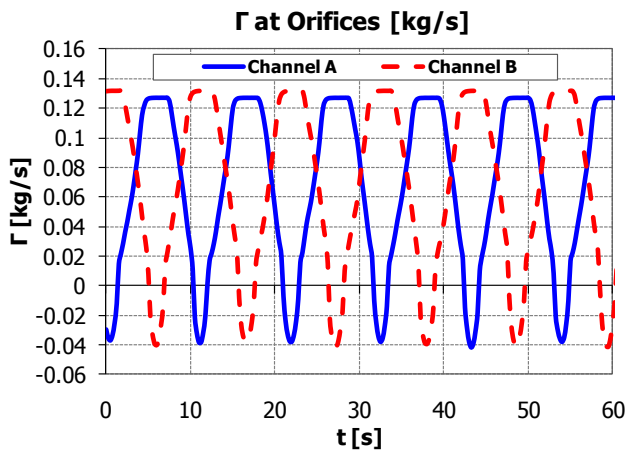


Fig. 3. Flow rate oscillations during fully developed instability. Data collected with:  $P = 83$  bar;  $T_{in} = 199$  °C;  $G = 597$  kg/m<sup>2</sup>s;  $Q = 99.3$  kW.

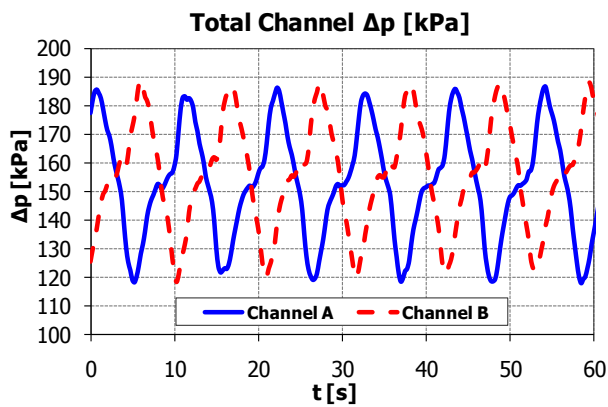


Fig. 4. Counter-phase pressure drop oscillations in the two parallel tubes. Data collected with:  $P = 83$  bar;  $T_{in} = 199$  °C;  $G = 597$  kg/m<sup>2</sup>s;  $Q = 99.3$  kW.

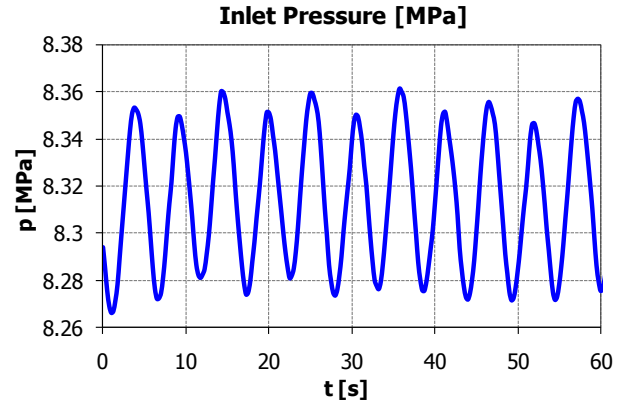


Fig. 5. System pressure oscillations in the inlet header. Data collected with:  $P = 83$  bar;  $T_{in} = 199$  °C;  $G = 597$  kg/m<sup>2</sup>s;  $Q = 99.3$  kW.

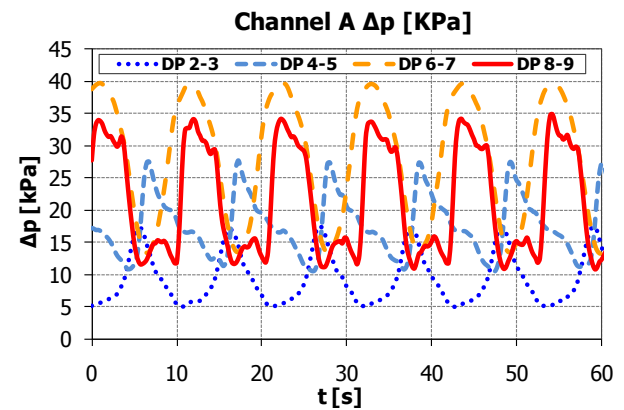


Fig. 6. Pressure drop oscillations in different regions of channel A: single phase (DP 2-3), low quality two-phase (DP 4-5), two-phase (DP 6-7 and DP 8-9). Data collected with:  $P = 83$  bar;  $T_{in} = 199$  °C;  $G = 597$  kg/m<sup>2</sup>s;  $Q = 99.3$  kW.

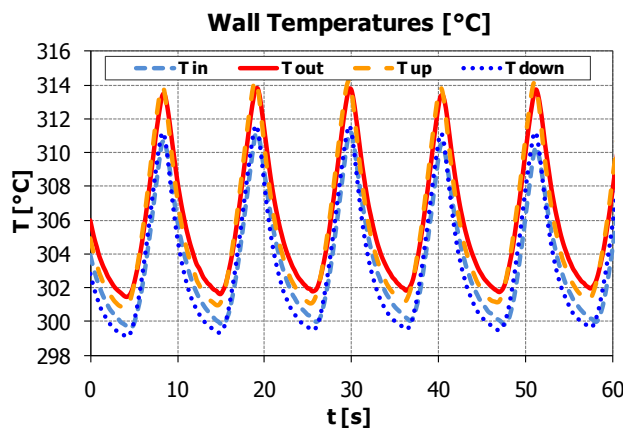


Fig. 7. Fluctuations of tube wall temperatures during DWOs. Data collected with:  $P = 83$  bar;  $T_{in} = 199$  °C;  $G = 597$  kg/m<sup>2</sup>s;  $Q = 99.3$  kW.

#### IV. EXPERIMENTAL RESULTS

For stability investigations, the aim is to find the regions of stable and unstable operation in the three-dimensional space given by channel flow rate  $\Gamma$ , thermal power  $Q$  and inlet subcooling  $\Delta h_{in}$  (in enthalpy units). A mapping of these regions in two dimensions is referred to as the stability map of the system (at a given pressure level). The stability boundary in the  $(\Gamma, Q, \Delta h_{in})$  space is a surface and can be represented only by a family of curves in any two-dimensional map. Thus, the adoption of dimensionless stability maps is useful to cluster the information on the dynamic characteristics of the system. The most used dimensionless stability map is due to Ishii and Zuber<sup>7</sup>. It is based on a subcooling number  $N_{sub}$  versus a phase change number  $N_{pch}$ . The phase change number is the ratio of the characteristic frequency of phase change  $\Omega$  to the inverse of a single-phase transit time in the system:

$$N_{pch} = \frac{\Omega}{\frac{V_{in}}{L}} = \frac{\frac{Q}{A \cdot L} \cdot \frac{v_{lv}}{h_{lv}}}{\frac{V_{in}}{L}} = \frac{Q}{\Gamma \cdot h_{lv}} \cdot \frac{v_{lv}}{v_l} \quad (1)$$

The subcooling number reads:

$$N_{sub} = \frac{\Delta h_{in}}{h_{lv}} \cdot \frac{v_{lv}}{v_l} \quad (2)$$

where all the thermodynamic properties are defined at the inlet pressure (within the lower header).

For the sake of completeness, some examples of typical stability maps obtained in case of straight vertical tube geometry are depicted in Fig. 8. Experimental data from the noteworthy work of Masini et al.<sup>6</sup> are retrieved, considering different configurations for the valves at inlet/outlet of the test section.

Conversely, Fig. 9, Fig. 10 and Fig. 11 show the stability maps obtained with the experimental data collected at the three pressure levels investigated in the present helical tubes facility. Error bars have been introduced following uncertainty analysis based on error linear propagation techniques<sup>8</sup>. The uncertainties of final dimensionless numbers within the maps have been computed combining the effects of the various measured quantities. Main effect is due to threshold power, following the uncertainties of measured electrical power, estimated thermal losses, as well as a term due to the discrete experimental procedure. Effect of pressure is also accounted for, by evaluating the maximum variation between the pressure recorded at instability inception with respect to the nominal pressure level. Pressure term is made apparent by the sensitivity of Eqs. (1), (2) on small pressure variations, which is considerably large at low pressure (such to overcome threshold power uncertainty)<sup>9</sup>.

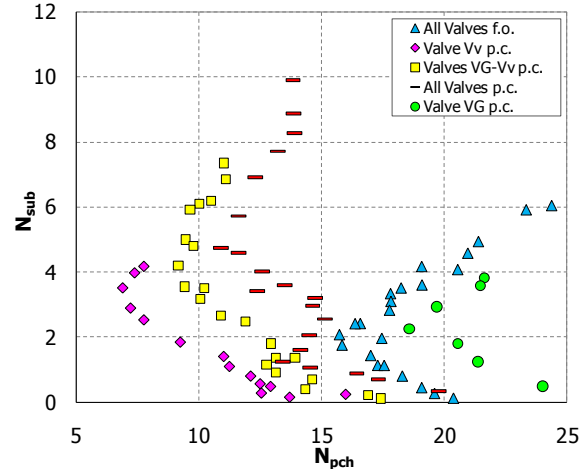


Fig. 8. Stability maps as retrieved from the experimental work of Masini et al.<sup>6</sup>, dealing with straight vertical tubes.  $P = 50$  bar;  $G = 364$  kg/m<sup>2</sup>s; Valves: VG inlet – Vv outlet. Valve positions: f.o. fully open – p.c. partially closed.

The three different curves depicted in each graph represent the instability thresholds for the three values of mass flux ( $G = 600$  kg/m<sup>2</sup>s,  $400$  kg/m<sup>2</sup>s and  $200$  kg/m<sup>2</sup>s), testing different inlet subcooling values. At 80 bar only two mass fluxes have been considered, because plant operations resulted difficult at low flow rates. As expected, the stability boundaries according to the various mass fluxes are almost overlapped. Thus, it is the ratio  $Q/\Gamma$  that determines the onset of instability once the characteristics of the channel and the inlet conditions are set. Fig. 12, Fig. 13 and Fig. 14 confirm, for the three pressure levels respectively, that a mass flow rate variation induces a proportional variation of the thermal power needed to trigger the instability. An increase in thermal power or a decrease in channel mass flow rate can cause the onset of DWOs; both effects increase the exit quality, which turns out to be a key parameter for boiling channel instability. In brief, the effects on instability of thermal power and mass flow rate do not show differences in the helical geometry when compared to the straight tube case (compare with Fig. 8).

Instead, it is interesting to focus the attention on inlet subcooling. It is well known from literature that an increase in inlet subcooling is stabilizing at high subcoolings and destabilizing at low subcoolings<sup>3</sup>. This behavior results in the classical “L shape” of the stability boundary, exhibited by all the dimensionless maps available in literature and referred to straight geometry<sup>6,7,10</sup> (Fig. 8). The present datasets with helical geometry confirm the stabilizing effect at high subcoolings. The experimental stability maps show indeed two different behaviors: (a) “conventional” at medium-high subcoolings, with iso-quality stability boundary and slight stabilization in the range  $N_{sub} = 3 \div 6$  (close to “L shape”); (b) “non-conventional” at low subcoolings, with marked destabilizing effects as inlet temperature increases and approaches the saturation value.

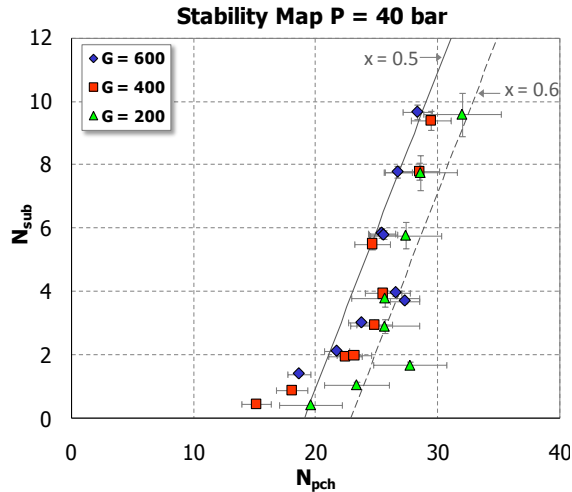


Fig. 9. Stability map obtained at system pressure  $P = 40$  bar and different mass fluxes ( $G = 600$  kg/m<sup>2</sup>s,  $400$  kg/m<sup>2</sup>s,  $200$  kg/m<sup>2</sup>s).

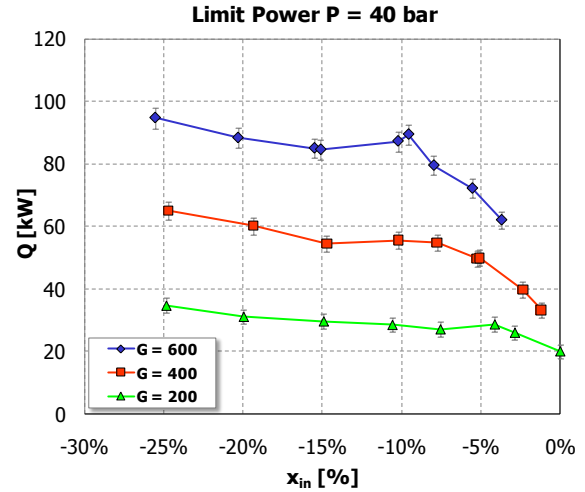


Fig. 12. Limit power for instability inception at  $P = 40$  bar as function of inlet subcooling and for different values of mass flux.

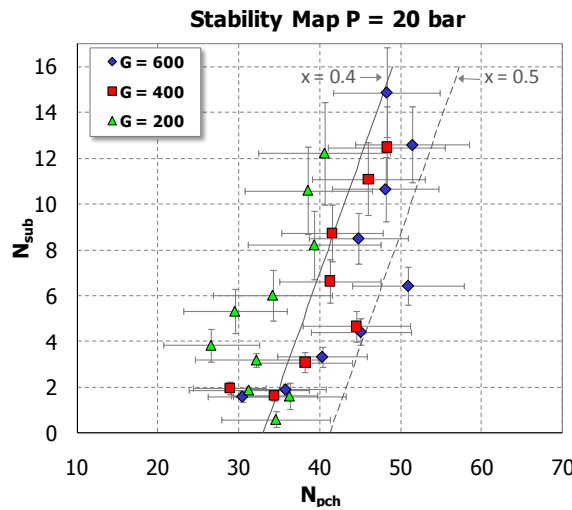


Fig. 10. Stability map obtained at system pressure  $P = 20$  bar and different mass fluxes ( $G = 600$  kg/m<sup>2</sup>s,  $400$  kg/m<sup>2</sup>s,  $200$  kg/m<sup>2</sup>s).

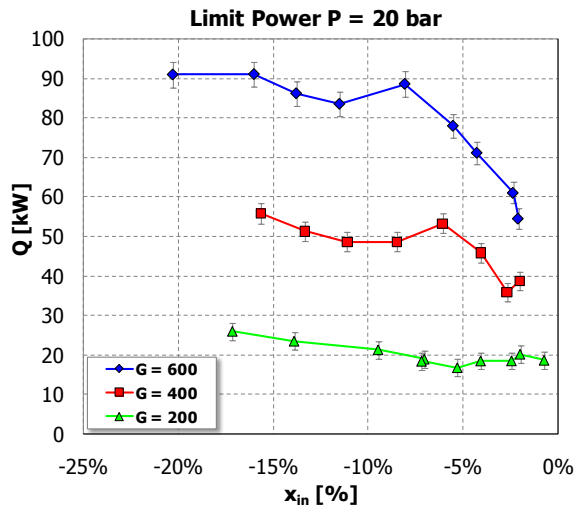


Fig. 13. Limit power for instability inception at  $P = 20$  bar as function of inlet subcooling and for different values of mass flux.

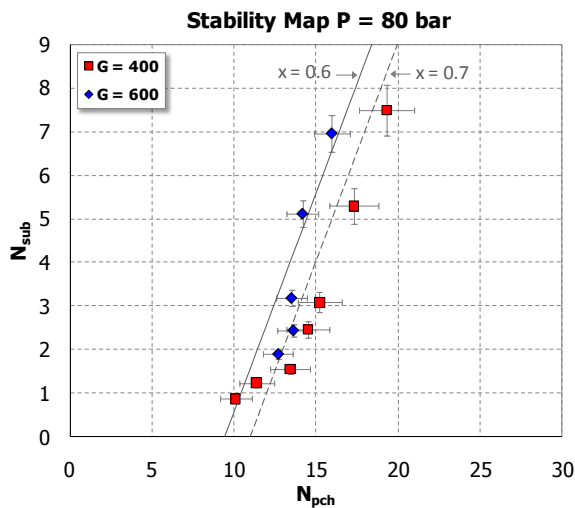


Fig. 11. Stability map obtained at system pressure  $P = 80$  bar and different mass fluxes ( $G = 600$  kg/m<sup>2</sup>s,  $400$  kg/m<sup>2</sup>s).

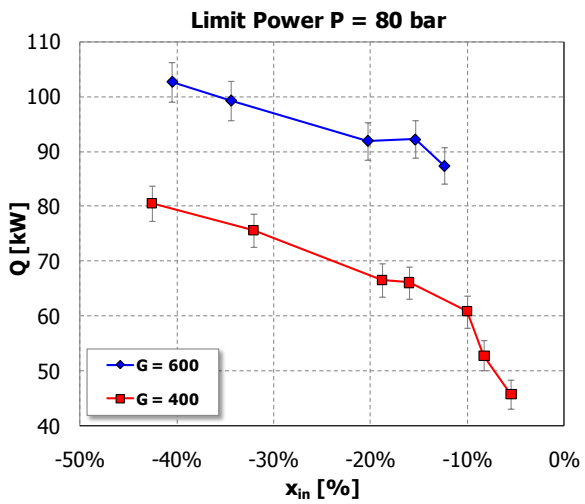


Fig. 14. Limit power for instability inception at  $P = 80$  bar as function of inlet subcooling and for different values of mass flux.

Such different behavior exhibited by the stability boundary at low subcoolings can be ascribed to the helical shape of the parallel channels and related centrifugal field effects on the thermal-hydraulics of two-phase flow. Also the full-scale length of the test section and the small inclination angle of the helix – affecting two-phase flow pattern – may explain the provided experimental results.

It is just noticed that at the lowest system pressure and lowest mass flux ( $P = 20$  bar and  $G = 200$  kg/m<sup>2</sup>s, see Fig. 10) the stability boundary shape is different from previous discussion and agrees more with classical behavior given by straight vertical tubes. As a matter of fact, the effect of inlet subcooling increase is stabilizing at high subcoolings, and destabilizing at low subcoolings. The centrifugal field – reasonably weak under these conditions – is such to make the peculiar effect of the helical geometry negligible.

#### IV.A. Effect of system pressure

System pressure was always found to be stabilizing, although pressure effect is less effective if compared with other system parameters<sup>3</sup>. Fig. 15 shows the limit power corresponding to the various pressure levels, fixed the mass flow rate in the system ( $G = 400$  kg/m<sup>2</sup>s). The higher is the pressure, the higher is the exit quality required for the onset of instability, hence the system is more stable. This concern is evident by considering the iso-quality lines reported in the stability maps (Fig. 9, Fig. 10 and Fig. 11). Thermal power behavior in Fig. 15 also confirms the subcooling destabilizing effect for small values of  $N_{sub}$ .

#### IV.B. Period of oscillations and transit time

DWOs are characterized by waves of heavier and lighter fluid which travel alternatively along the boiling channel<sup>3</sup>. Two perturbations are required for each cycle. Accordingly, the period of oscillations should be of the order of twice the mixture transit time. As a matter of fact, literature results report a period of oscillation  $T$  almost equal to twice the mixture transit time  $\tau$  at high inlet subcoolings, and a reduction of  $T/\tau$  ratio by reducing the subcooling number<sup>3</sup>. In this respect, mixture transit time is considered calculated with classical homogeneous flow theory, by adding single-phase region transit time  $\tau_{1\phi}$  and two-phase region transit time  $\tau_{2\phi}$ , as in<sup>3,6</sup>:

$$\tau = \tau_{1\phi} + \tau_{2\phi} = \frac{\overline{\rho_{in}} \Delta h_{in}}{Q'''} + \frac{h_{fg}}{Q'''' v_{fg}} \ln \left( 1 + \frac{v_{fg}}{v_f} x_{ex} \right). \quad (3)$$

With some algebra, Eq. (3) can be rearranged as:

$$\tau = \frac{ALh_{fg}}{Q} \left[ -\overline{\rho_{in}} x_{in} + \frac{1}{v_{fg}} \ln \left( 1 + \frac{v_{fg}}{v_f} x_{ex} \right) \right]. \quad (4)$$

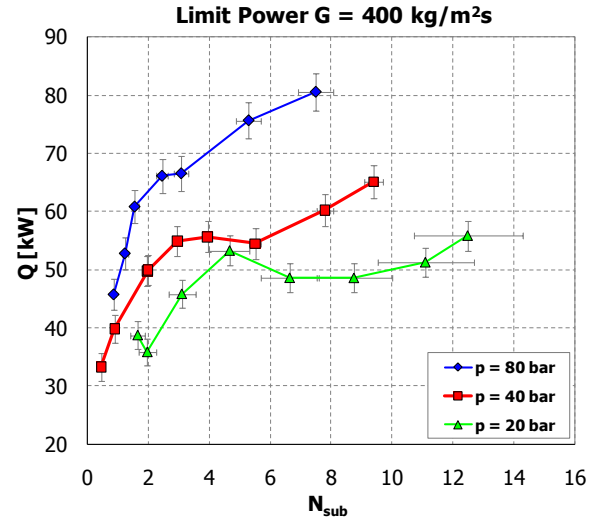


Fig. 15. Limit power for instability inception at  $G = 400$  kg/m<sup>2</sup>s as function of the subcooling number and at different pressures.

The experimental results collected at SIET labs show a completely different trend. The period of oscillations to transit time ratio is found to be very low at high inlet subcoolings, moreover it grows by reducing the subcooling number  $N_{sub}$ . The period of oscillations (Fig. 16) is rather independent on inlet subcooling, whereas it increases as the mass flux is lower. Accordingly,  $T/\tau$  ratio (Fig. 17) – pretty constant following mass flux variations – results considerably lower than one ( $\sim 0.5$ ) at high inlet subcoolings (when the fluid transit time in the heated channel is higher due to the long single-phase region), whereas it increases up to a value of nearly two as the inlet temperature approaches the saturation.

Up to the Authors knowledge, as well as from the helical geometry, the discussed behavior seems to be induced also by the peculiar length of the test section and by the presence of an unheated riser above.

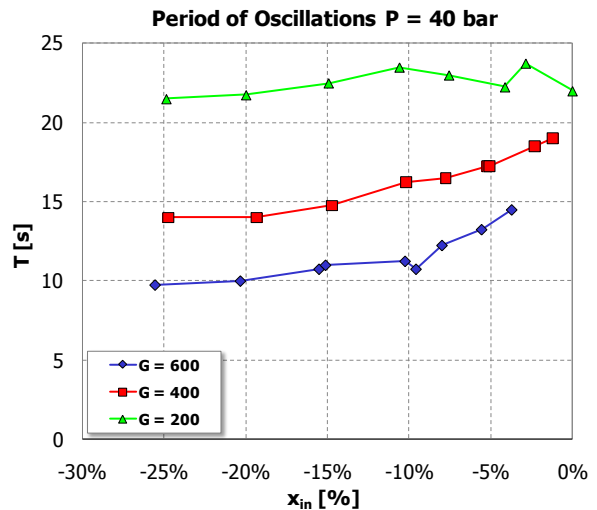


Fig. 16. Period of oscillations at  $P = 40$  bar as function of inlet subcooling and for different values of mass flux.



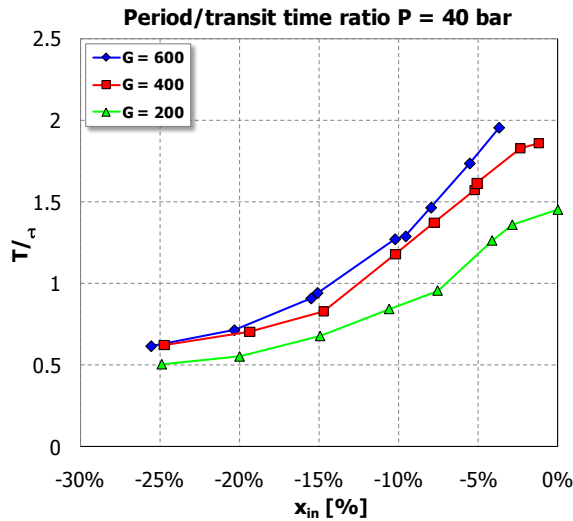


Fig. 17. Period of oscillations to transit time ratio at  $P = 40$  bar as function of inlet subcooling and for different values of mass flux.

#### IV.C. Effect of inlet throttling

It is well known that a concentrated pressure drop located at channel inlet is stabilizing. Therefore, the stability of the system was investigated after a closure of the inlet valves (valve loss coefficient characterized by the value  $k_{in} = 90$ ). The results, depicted in Fig. 18 ( $P = 40$  bar and  $G = 400$  kg/m<sup>2</sup>s), confirm the stabilizing effect of a concentrated pressure drop at the inlet of the channel, even though the difference between the two curves becomes almost negligible at low  $N_{sub}$  values.

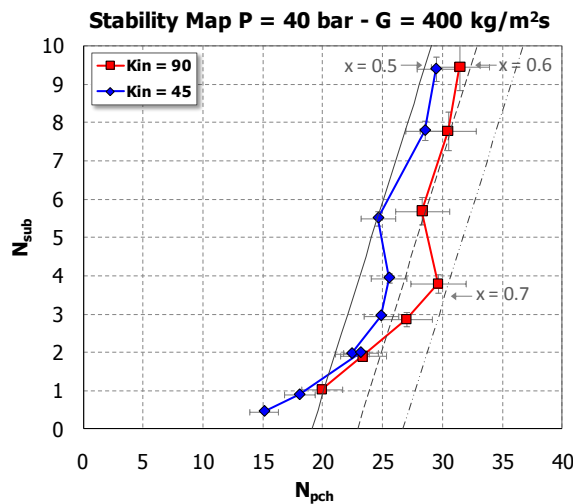


Fig. 18. Effect of inlet throttling on instability threshold at system pressure  $P = 40$  bar and mass flux  $G = 400$  kg/m<sup>2</sup>s.

#### IV.D. Ledinegg type instabilities

The final Section of the paper is dedicated to Ledinegg type instability. Ledinegg flow excursions were observed during test runs at the lowest pressure level ( $P = 20$  bar),

the highest mass flux ( $G = 600$  kg/m<sup>2</sup>s), and higher inlet subcooling values ( $x_{in} < -15\%$ ). Ledinegg type instabilities occur when a heated channel operates in the negative slope region of the pressure drop versus flow rate curve (channel characteristics). In this respect, the boundary conditions of constant-pressure-drop given by parallel channels act as a flat pump external characteristics, forcing each channel into a wide flow excursion up to the reaching of new operating points on the internal characteristics.

Fig. 19 shows the flow rate evolution in each channel in presence of a Ledinegg type instability. Flow excursion is evident, as Channel A flow rate increases. On the contrary, flow rate in Channel B reduces proportionally to preserve the imposed total mass flow rate. Constant total pressure drop condition is respected across the two tubes. Ledinegg instability occurrence showed to be critical since an anticipated DWO onset was recorded in the channel with lower flow rate (Channel B in this case), following small increases of supplied thermal power. Indeed, increase of thermal power permitted to leave the Ledinegg instability region, damping out the flow excursion.

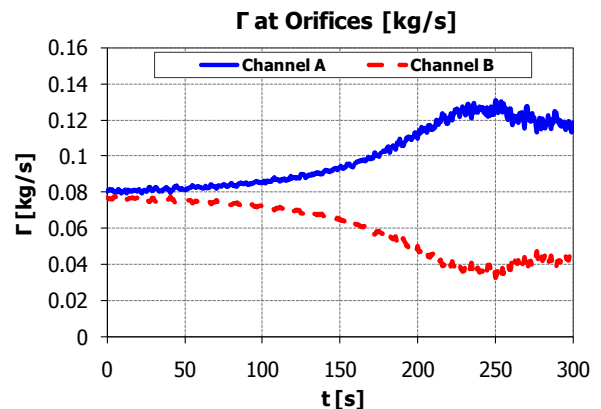


Fig. 19. Flow rate recorded in the two channels during a Ledinegg transient.

Data collected with:  $P = 24$  bar;  $T_{in} = 134$  °C;  $G = 601$  kg/m<sup>2</sup>s. Transient to  $Q = 50$  kW (electrical power supplied per tube).

## V. CONCLUSIONS

An experimental investigation on DWOs in helically coiled parallel channels has been presented in this paper. A full-scale open-loop experimental facility was specifically built and operated at SIET labs in Piacenza (Italy), comprising two helical tubes (connected by means of two common headers) in simulation of the helically coiled steam generator of a GenIII+ SMR.

Main goal of the experiments has been to study the influence of the helical geometry on instability thresholds in parallel channels, as well as to provide a thorough threshold database useful for model validations.

The effects of system pressure, flow rate and inlet subcooling on the power at the onset of instability have

been investigated, clustering the data in dimensionless stability maps. The effects of thermal power and mass flow rate in determining the channel exit quality triggering the instability are consistent with classical DWO theory in straight tubes. On the contrary, specific features have been highlighted when considering the effects of inlet subcooling. With respect to literature results, the destabilizing effect of an increase of inlet subcooling at low subcooling values is not apparent. Conversely, the subcooling maintains its stabilizing effect, which increases indeed as the inlet temperature approaches the saturation value. Discrepancies with respect to classical DWO theory have been also observed in terms of period of oscillations and period-over-transit time ratio. The period of oscillations is rather independent on inlet subcooling, and the period to transit time ratio increases by increasing the inlet temperature.

Mentioned deviations from literature results have been preliminarily ascribed to the helical geometry and the peculiar geometrical characteristics of the test section, even though a detailed theoretical study on the concern has not been finalized yet. In this framework, modeling activities are underway through the development of dynamic models and numerical simulations with system codes.

At the end, effect of inlet throttling and appearance of Ledinegg type instabilities have been discussed. The first one is rather weak for the parallel channel system investigated; only a strong increase of the inlet throttling – with concentrated pressure drop term such to equalize distributed pressure drop term along the channel – should permit to avoid the inception of the instability. More experiments are also needed to better characterize the operating regions affected by Ledinegg instabilities.

#### NOMENCLATURE

|            |   |
|------------|---|
| $A$        | tube area [m <sup>2</sup> ]                           |
| $DP$       | differential pressure [kPa]                           |
| $G$        | mass flux [kg/m <sup>2</sup> s]                       |
| $h$        | enthalpy [kJ/kg]                                      |
| $k$        | valve loss coefficient [-]                            |
| $L$        | tube length (heated zone) [m]                         |
| $N_{pch}$  | phase change number [-]                               |
| $N_{sub}$  | subcooling number [-]                                 |
| $P$        | pressure [bar]  |
| $Q$        | thermal power [kW]                                    |
| $Q'''$     | thermal power per unit of volume [kW/m <sup>3</sup> ] |
| $t$        | time [s]  |
| $V$        | velocity [m/s]  |
| $v$        | specific volume [m <sup>3</sup> /kg]                  |
| $x$        | thermodynamic quality [-]                             |
| $\Delta p$ | pressure drops [kPa]                                  |
| $\Gamma$   | mass flow rate [kg/s]                                 |
| $\tau$     | heated channel transit time [s]                       |
| $\Omega$   | characteristic frequency of phase change [1/s]        |

#### ACRONYMS

|      |   |
|------|---|
| DWO  | Density Wave Oscillation  |
| IRIS | International Reactor Innovative and Secure   |
| LOCA | Loss Of Coolant Accident  |
| PWR  | Pressurized Water Reactor   |
| SG   | Steam Generator   |
| SIET | Società Informazioni Esperienze Termoidrauliche<br>(company for information on thermal-hydraulic experimentation) |
| SMR  | Small-medium Modular Reactor  |

#### REFERENCES

1. L. Santini, A. Cioncolini, C. Lombardi, M.E. Ricotti, “Two Phase Pressure Drops in a Helically Coiled Steam Generator”, *International Journal of Heat and Mass Transfer*, **51**, 4926-4939 (2008).
2. L. Santini, D. Papini, M.E. Ricotti, “Experimental Characterization of a Passive Emergency Heat Removal System for a Gen III+ Reactor”, *Science and Technology of Nuclear Installations*, **Vol. 2010**, doi: 10.1155/2010/864709, 12 pages (2010).
3. G. Yadigaroglu, “Two-Phase Flow Instabilities and Propagation Phenomena”, In: J.M. Delhaye, M. Giot, M.L. Riethmuller, *Thermohydraulics of two-phase systems for industrial design and nuclear engineering*, 353-396, Hemisphere Publishing Corporation, Washington (1981).
4. S. Kakaç and B. Bon, “A Review of Two-Phase Flow Dynamic Instabilities in Tube Boiling Systems”, *International Journal of Heat and Mass Transfer*, **51**, 399-433 (2008).
5. P. Saha, M. Ishii, N. Zuber, “An Experimental Investigation of the Thermally Induced Flow Oscillations in Two-Phase Systems”, *Journal of Heat Transfer*, **98**, 616-622 (1976).
6. G. Masini, G. Possa, F.A. Tacconi, “Flow Instability Thresholds in Parallel Heated Channels”. *Energia Nucleare*, **15**, 12, 777-786 (1968).
7. M. Ishii and N. Zuber, “Thermally Induced Flow Instabilities in Two-Phase Mixtures”, *Proc. of the 4<sup>th</sup> International Heat Transfer Conference*, vol. 5, paper B5.11, Paris, France (1970).
8. R.J. Moffat, “Describing the Uncertainties in Experimental Results”, *Experimental Thermal and Fluid Science*, **1**, 3-17 (1988).
9. D. Papini, “Modelling and experimental investigation of helical coil steam generator for IRIS Small-medium Modular Reactor”, *PhD Thesis*, Politecnico di Milano, Department of Energy, cycle XXIII, Milan, Italy (2011).
10. W. Ambrosini, P. Di Marco, J.C. Ferreri, “Linear and Nonlinear Analysis of Density Wave Instability Phenomena”, *International Journal of Heat and Technology*, **18**, 1, 27-36 (2000).